Energy 183 (2019) 1061–1074

Contents lists available at ScienceDirect

Energy

journal homepage: www.elsevier.com/locate/energy

Power variability of tidal-stream energy and implications for electricity supply

Matt Lewis [a, *], James McNaughton [d], Concha Márquez-Dominguez [a], Grazia Todeschini [b], Michael Togneri [b], Ian Masters [b], Matthew Allmark [c], Tim Stallard [e], Simon Neill [a], Alice Goward-Brown [a], Peter Robins [a]

[a] Bangor University, UK
[b] Swansea University, UK
[c] Cardiff University, UK
[d] University of Oxford, UK
[e] Manchester University, UK

ARTICLE INFO

Article history:
Received 20 March 2019
Received in revised form
20 June 2019
Accepted 29 June 2019
Available online 1 July 2019

Keywords:
Tidal energy
Prediction
Turbulence
Power quality
Orkney
Resource characterisation

ABSTRACT

Temporal variability in renewable energy presents a major challenge for electrical grid systems. Tides are considered predictable due to their regular periodicity; however, the persistence and quality of tidal-stream generated electricity is unknown. This paper is the first study that attempts to address this knowledge gap through direct measurements of rotor-shaft power and shore-side voltage from a 1 MW, rated at grid-connection, tidal turbine (Orkney Islands, UK). Tidal asymmetry in turbulence parameters, flow speed and power variability were observed. Variability in the power at 0.5 Hz, associated with the 10-min running mean, was low (standard deviation 10–12% of rated power), with lower variability associated with higher flow speed and reduced turbulence intensity. Variability of shore-side measured voltage was well within acceptable levels (~0.3% at 0.5 Hz). Variability in turbine power had <1% difference in energy yield calculation, even with a skewed power variability distribution. Finally, using a "t-location" distribution of observed fine-scale power variability, in combination with an idealised power curve, a synthetic power variability model reliably downscaled 30 min tidal velocity simulations to power at 0.5 Hz ($R^2 = 85\%$ and ~14% error). Therefore, the predictability and quality of tidal-stream energy was high and may be undervalued in a future, high-penetration renewable energy, electricity grid.

1. Introduction

It is vital that countries convert to a sustainable low-carbon electricity system, and yet many renewable energy sources exhibit variability in power output over a range of time-scales with low predictability compared with traditional electricity sources [1]. One of the key challenges integrating renewable energy into a guaranteed high-quality electricity supply is to ensure electricity supply matches demand (e.g. Refs. [2,3]) – thus, reducing expensive storage and system control measures [4–6].

There are many renewable energy sources, some of which are well established and dispatchable (e.g. hydro-electric and biomass), however recent interest in deploying a large amount of renewable energy sources (e.g. high penetration of renewable energy in a power grid) that are less dispatchable (i.e. the resource, thus electricity, is not always present) is discussed in context to the immature/developing tidal-stream energy industry. Fine-scale variability in renewable energy supplies arise from, for example, the passing of clouds for solar PV and gustiness for wind energy; it is this renewable energy temporal variability that this paper discusses in context to tidal-stream energy. The predictability of clouds and therefore the persistence of solar energy is considered low [7,8], whilst turbulent fluctuations in wind speed (which we experience as gusts) are known to directly affect wind energy generation through changing wind turbine rotor speed [7,9]. The variability of tidal energy is often quoted as "low" in comparison to some other forms of renewable energy (e.g. Refs. [10,11]), therefore this article will explore fine-scale tidal-stream energy and implications for electricity supply.

* Corresponding author.
E-mail address: m.j.lewis@bangor.ac.uk (M. Lewis).

https://doi.org/10.1016/j.energy.2019.06.181

Energy control systems are needed to match supply with demand; hence, power utilities and transmission system operators are concerned with the reported temporal variability of renewable energy power [12]. Different solutions are available to mitigate this concern, for example: the use of 'spinning reserve' when demand exceeds generation, and curtailment of energy sources when generation exceeds demand – as well as more sophisticated control strategies (see Refs. [13–15]). These solutions result in significant drawbacks: (1) spinning reserves include devices such as diesel generators and, therefore, they are potentially polluting and costly. (2) Curtailment of energy sources means a reduced income for the owners and may potentially discourage further investment in renewable resources. (3) Energy storage may be an alternative solution; however, large-scale storage for power grids is presently not widely deployed. Therefore, as a result of the variability of renewable energy resources, higher costs are expected to be incurred in a future low-carbon electricity system [3,16,17].

In addition to variability of electricity supply, the shift of generation from fossil-fuelled energy sources to renewable generation creates a concern in relation to system inertia. Inertia of a power system is defined as the ability of a system to oppose changes in frequency, due to the kinetic energy stored in the rotating masses in synchronous generators. In an AC system, any imbalance between electricity supply and demand will result in a change to the frequency; for example, when electricity demand exceeds generation, the system frequency will decrease. As a result, utilities and transmission system operators are concerned that a continuous decrease in system inertia will compromise grid stability (e.g. maximum deviation of 1% is tolerated at a nominal frequency of 50 Hz in the UK). Renewable sources that are decoupled from the grid, by means of power converters (e.g. solar-PV), do not contribute to system inertia unless specific requirements are introduced. For example, in Germany and Denmark (e.g. Refs. [3,14]), wind energy is contributing to system inertia. Therefore, tidal energy could also contribute to regulation of electricity supply.

The periodicity of the tide allows accurate tidal predictions far into the future using harmonic analysis or ocean modelling techniques (e.g. Ref. [18]). For hydrokinetic turbines, which are used in tidal-stream electricity generation, the power (P) depends on the cube of velocity of the current ($\overline{U}$) at the site, the density of the fluid (ρ), the swept rotor area (A) and its design or "efficiency" (Cp): $P = 0.5*\rho*A*Cp*\overline{U}^3$ [Eq. 1]. Following linear wave theory for a semi-diurnal system (like the UK), the resource ($\overline{U}$) is above 50% of peak flow for 67% of the tidal cycle, with the timing of peak flow advances 25.2 min each tidal cycle. Therefore, tidal energy is often publicised as a predictable and "high-quality" renewable energy source (e.g. Ref. [10]).

In strongly semi-diurnal systems, the largest tides of the fortnightly "spring-neap" cycle always occur at a similar time of day (see [62]), due to the interaction of the phase-locked solar constituent (S2) and the lunar constituent (M2). Furthermore, the progression of the tidal wave, as it travels around the UK coastline, means a phase difference in the timing of peak tidal electricity production along a coastline could be exploited [19]; for example, three tidal power stations 120° out-of-phase to one another would produce a constant amount of power over a tidal cycle for regions with a suitable coastline (it is unknown if such tidal systems exists elsewhere in the world as research in this area is preliminary, see Ref. [20]). The predictability of tidal power could therefore be advantageous for baseload electricity within the UK's national grid, because arrays of tidal-stream turbines could be strategically sited along a coastline to compensate tidal phase differences and produce a firm baseload of electricity [11,21].

The spatio-temporal variability of tidal currents can be simulated with ocean models for tidal energy resource assessments (e.g. Ref. [10]). Simulated velocities are typically resolved every 15–60 min. The turbulent closure schemes applied in such models do not resolve realistic turbulent fluctuations and, hence, tidal power fluctuations. Turbulence is the fluctuation of velocity (u') within a time-mean window ($\overline{U}$); thus velocity at a point in time (u_t) is expressed as $u_t = \overline{U} + u'$. Turbulence at highly energetic tidal-stream sites is known to be relatively high [22]; for example, between 12% and 13% turbulence intensity (TI) at turbine hub–height [23], with differences noted between the flood and ebb tidal phases and surface-wave enhanced turbulence effects [24,25].

Turbulent loadings [26,27] and turbulence effects on thrust and power efficiency [28], have rightly been a focus of research in tidal energy. However, as the industry moves towards commercialization and the deployment of grid-connected devices [29], understanding the fine-scale current speed variability (i.e. turbulence) effects on electricity quality is therefore required; for both the development of the industry and integration of renewable energy at both national and micro-grid scales. Turbulence intensity at wind energy sites has been measured between 10% and 20% [30–33] and, therefore, wind turbulence is hypothesised to be slightly higher than turbulence at tidal energy sites [34,35]. The combination of slightly lower turbulence intensities at tidal-energy sites than wind sites, with the density of sea-water being ~800 times larger than air (see Eq. 1), suggests that fine-scale variability of tidal-stream energy should be lower than wind energy.

This paper aims to characterize tidal-stream power variability and develop a method that can downscale resource model information to efficiently predict electricity production for system operators. Using a unique 1 MW tidal-stream turbine data set, described in Section 2, we analysed the variability of electricity and power within a running-average time window (Section 3). Our results (Section 4) present the first characterisation of the quality of tidal-stream generated electricity, together with a method to downscale broad-scale (30 min resolution) model data to predict electricity production at 0.5 Hz frequency. Hence, we communicate the value of tidal-stream energy in both micro-grid and national-grid renewable electricity systems (Section 5).

2. Case study and data

The tidal-stream energy resource of Orkney (UK) is one of the largest worldwide, recognized by the development of the European Marine Energy Centre (EMEC) full-scale tidal test site – where the tidal-stream energy device analysed in this study was located. The region has been extensively studied (e.g. Ref. [36]), and a number of models exist for the region; for example, that of [37] which will be applied in Section 4. The tidal wave takes around 2.5 h to propagate in a clockwise direction around the Orkney Islands, which generates a strong pressure gradient flow through the Pentland Firth and the Firths of Orkney - tidal straits which link the Eastern-north Atlantic to the North Sea (see Fig. 1). Tidal currents in the Firths of Orkney exceed 3 m/s in many locations, with water depths also suitable for the first generation of tidal turbine developments [36]; see Fig. 1.

An 18 m diameter 1 MW tidal-stream turbine, was deployed as part of the ETI funded ReDAPT project, in the Fall of Warness at the EMEC site (see Fig. 1). Real time generator power (measured behind the generator within the nacelle) and shore side voltage (measured after the shore transformer) were measured at 50 Hz and 10 Hz, respectively. Power weighted rotor-averaged velocity and tidal current speed, based on ADCP measurements taken at hub height (downstream, i.e. southwest, of the turbine), was measured at

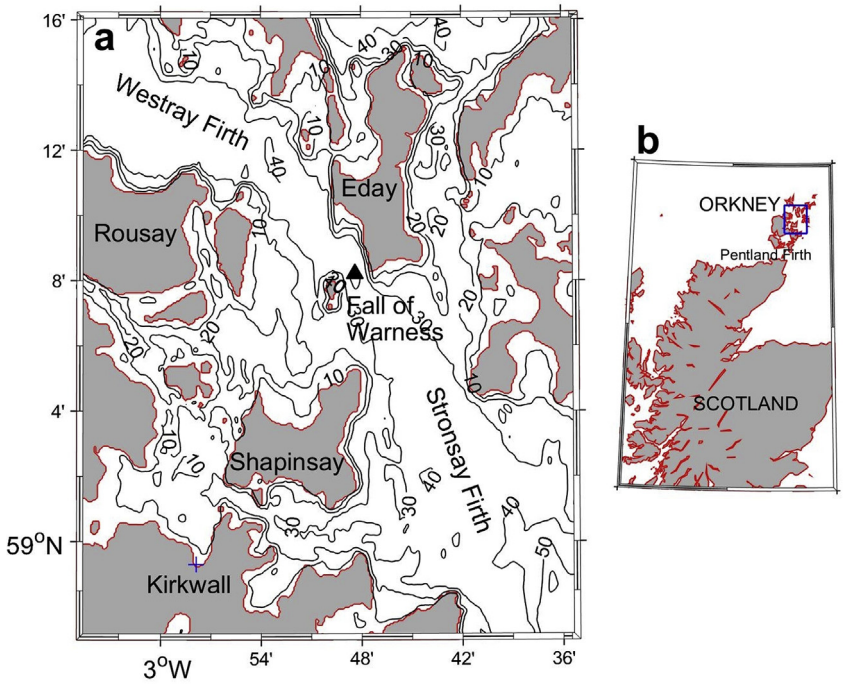

Fig. 1. The location of the Fall of Warness in the Orkney Islands (panel a), in Scotland, UK (panel b) where the EMEC site is, and a grid-connected 1 MW tidal-stream turbine was installed.

0.5 Hz. The electricity generated, measured power and hub height current speed were recorded for a full tidal cycle during two dates with similar spring tidal conditions: 26 October 2014 and 26 Nov 2014. Further details of the data are given in McNaughton [38] and Ahmed et al. [39] and flow data is available via the University of Edinburgh's data share (http://redapt.eng.ed.ac.uk/) - see Sellar and Sutherland [40].

Data was provided by GE Renewable Energy and has been normalised to protect commercial sensitivity. Therefore, figures are presented in this publication as percentages relative to 20% above the stated capacity (i.e. maximum power of device, *Pr*, in order to ensure a 1 MW rated power at the shore connection) and rated velocity (*Ur*), when the instantaneous velocity (u_t) is predicted to provide instantaneous power (P_t) at the rated turbine capacity ($P_t = Pr$). Therefore, all data is presented as a percentage relative to the value at rated power: this means we express velocity and power respectively as $\left(u_t/_{Ur}\right) \times 100\%$ and $\left(P_t/_{Pr}\right) \times 100\%$.

3. Method and preliminary analysis

All time-series data were linearly interpolated to a common time-series at a frequency of 0.5 Hz. Some uncertainty in the synchronicity of data-series (of the order of seconds) was noted (e.g. Ref. [38], but this will not affect our analysis as we explore variability from a mean value within averaging windows of the order of minutes to hours. The interpolated 0.5 Hz time-series of tidal-stream turbine power, shore-side voltage, and current velocity (at turbine hub height) allows an investigation into the fine-scale temporal variability of tidal-stream energy and potential causes (i.e. mean flow speed, turbulence and waves). Characterisation of the distribution of fine-scale turbine power variability, relative to the time-averaged mean (including sensitivity test to window choice), was performed. The fitted distribution of fine-scale turbine power variability allows a statistical method to down-scale tidal-stream hydrodynamic resource model information to fine-scale predictions of resource– which is presented in Section 4.

The 0.5 Hz (2 cycles per second) time-series of hub height tidal current velocity and tidal turbine shaft-power is shown in Fig. 2. The fine-scale temporal variability of tidal current and power are highlighted in Fig. 2, when compared with 30-min running means (black line of Fig. 2). The broader temporal variability of the resource appears to be accurately captured using hydrodynamic tidal resource models (e.g. Ref. [10], whilst the fine-scale variability of tidal-stream power is both novel and substantive (see Figs. 2 and 3). The fine-scale variability of tidal-stream power is clearly shown in the power curve of Fig. 3, comparing the 0.5 Hz measured power curve with an idealised power curve typically used in resource estimation and 30-min hydrodynamic model data [10]. This fine-scale variability in tidal-stream energy, the focus of this study, is crucial to understand because it allows systems to be designed to ensure renewable electricity can be useful to end users. Moreover, the fine-scale variability of Fig. 2 may be important for uncertainty quantification in resource estimation; thus, improving investor confidence in power curve estimation (Fig. 3).

It should be noted how the idealised power curve (red line of Fig. 3) is similar to the power observed at 0.5 Hz, even though the idealised power curve is based on a different device deployed in a very different tidal environment (Strangford Lough, see Ref. [10]) and applies 30-min hydrodynamic model data for current speed (see Eq. 1). Therefore, broader-scale and turbulence scales of velocity fluctuations, and the subsequent power captured by the turbine, is the difference between the red line and the black dots of Fig. 3. Finer-scale fluctuations in the 30-min mean velocity (x-axis of Fig. 3) clearly result in fluctuations in power (e.g. see Eq. 1), both above and below the red line as the 30-min average velocity is represented in Fig. 3 (hence the observed 2s normalised power of Fig. 3 are above and below the red line). Some data showed no power being measured during high velocity values (~90% to 130% of rated velocity; Fig. 3) – perhaps due to variability in velocity

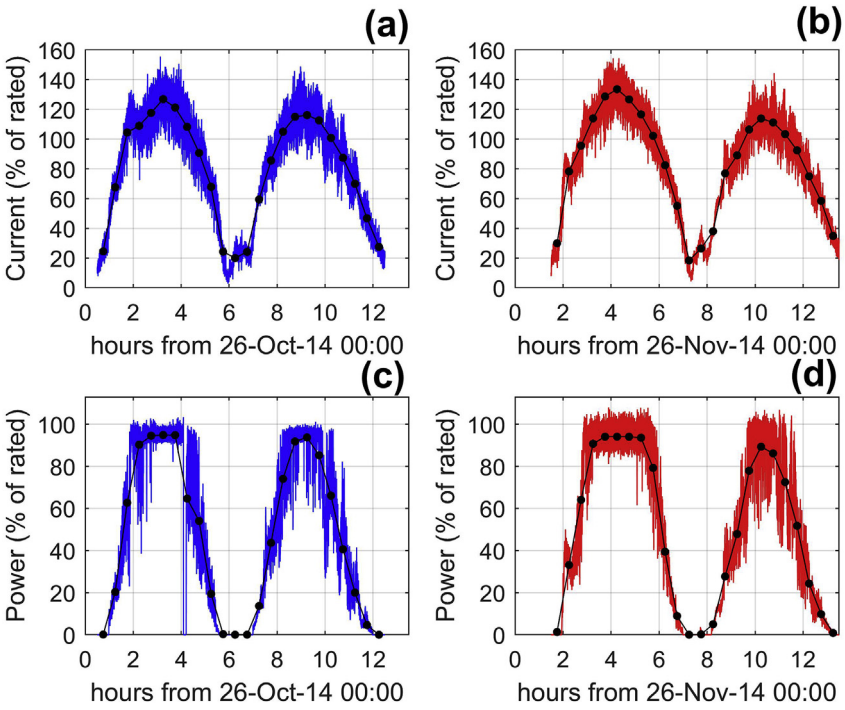

Fig. 2. The 0.5 Hz hub height tidal current and tidal turbine power, normalised to the rated power conditions and with a 30 min moving averaging (black line), for a tidal cycle in October 2014 (panel a and c) and November (panel b and d).

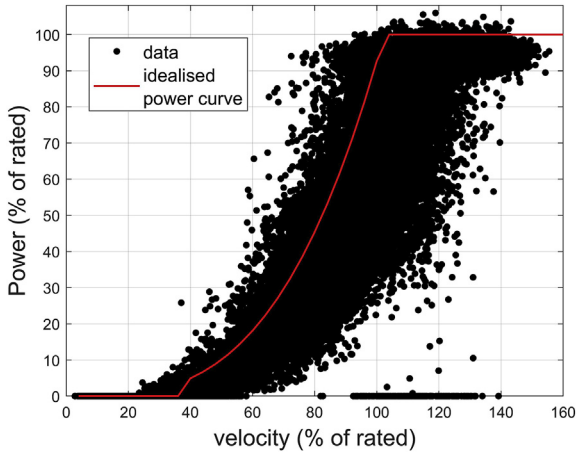

Fig. 3. The normalised 0.5 Hz measured power curve for the two tidal cycles in 2014 compared to an idealised power curve (red line of [10]) used in hydrodynamic model resource estimation. (For interpretation of the references to colour in this figure legend, the reader is referred to the Web version of this article.)

direction resulting in turbine stall. Values of power above 100% were also recorded in Fig. 3, due to the device rating being associated with the shoreside power rather than the turbine rotor shaft power, and hence much data at ~95% power above rated velocity.

Averaged spectra of the 0.5 Hz data are presented using Fast Fourier Transform (FFT) in Fig. 4, with power and velocity normalised. These are obtained by computing separate spectra for each hour-long subset of the data record, with a half-hour overlap between subsets and applying a Hann window to prevent aliasing. Although this FFT analysis has limitations, the effect of waves in oceanographic data such as this is routinely analysed with FFT [41] and a clear mode of oscillation is present in Fig. 4 during a large wave event. There is no significant periodicity to the fine-scale variability with the exception of the October time-series: the peak visible in both the velocity (panel a) and power (panel c) around 10s (10^{-1} Hz) coincides with a large wave event. Wave data was taken from the ERA interim hindcast data [42] for the corresponding model cell, and indicates a daily averaged offshore significant wave height of ~7 m and mean period of ~10 s for the 26-Oct-14. The apparent effect of waves to power is interesting, and Fig. 4 implies that the turbine has been able to extract some additional energy from the presence of waves, but quantifying this effect is beyond the scope of this paper.

To test the sensitivity of our analysis to the choice of averaging window, a Kolmogorov-Smirnov test (KS) for goodness of fit (see Ref. [43]) was applied with the null hypothesis (H) that the two data-series groups come from the same distribution (giving an associated P value of confidence in the result). No difference in our results was found when using sub-hourly time-averaging windows: see Table 1. Therefore, based on the results of Table 1, we find the variability in flood and ebb tidal power significantly different, but the October and November dates can be grouped together for analysis if a running mean, of the order of minutes, is used.

Differences in the power curve with various moving-average windows, and the associated error (difference in the sum of power in the two tidal cycles between the 0.5 Hz and the time-averaged power time-series), is shown in Fig. 5. The results of Table 1 and Fig. 5, along with previous studies of turbulence intensity quantification at tidal-stream energy sites [23], voltage variability [44, 45] and fine-scale wind-power variability [16], led to a 10 min moving average window being used for analysis in our study (which averages out any wave influenced oscillations) - with data grouped for flood and ebb tides.

The variability of power, relative to the 10-min mean (δP), is also expressed as a percentage relative to the mean ($\delta power$) so the distribution of power variability relative to a time-averaging window can be achieved. This variability in observed power, relative to the time-averaging window ($\delta power$), has units of percentage

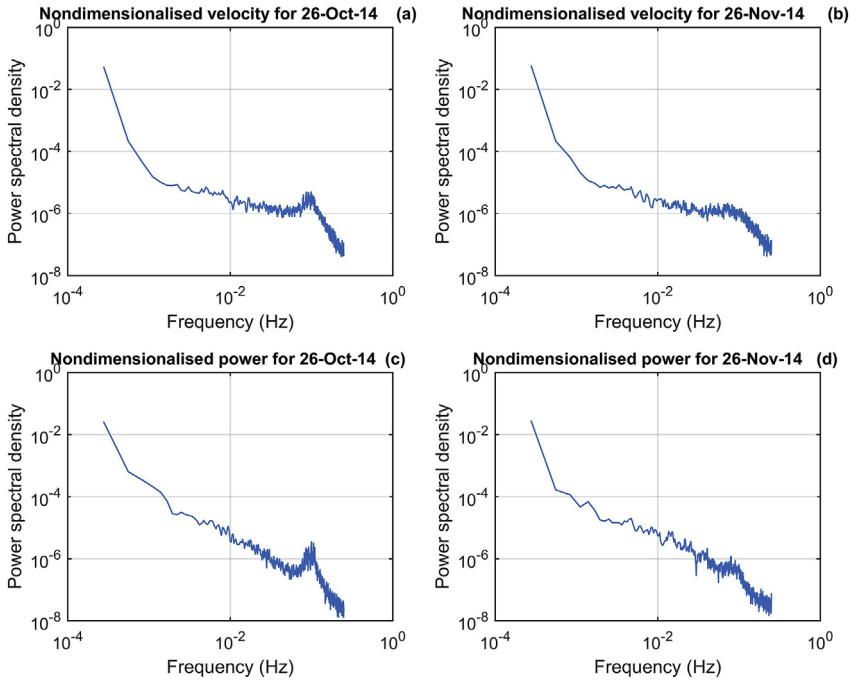

Fig. 4. Fast Fourier Transform analysis of the normalised and smoothed 0.5 Hz hub height tidal velocity (U) and turbine measured power (P) for two tidal cycles: one on 26-Oct-14 (panels a and c) and one 26-Nov-14 (panels b and d).

Table 1
Similarity of distributions from grouped tidal-stream turbine data. The result of a two-sample Kolmogorov-Simrnov test (at 5% significance level); displayed as H (the result given as diff or same for the two groups tested), P (asymptotic p-value between 0 and 1), and KS (the test statistic as critical value).

		Velocity (various running means)					Power (various running means)				
Two groups tested		raw 2s data	10 m mean	15 m mean	30 m mean	60 m mean	raw 2s data	10 m mean	15 m mean	30 m mean	60 m mean
2 dates (all tides)	H	**diff**	**same**	**same**	**same**	**same**	**diff**	**same**	**same**	**same**	**same**
	P	0.00	1.00	1.00	1.00	1.00	0.00	1.00	1.00	1.00	1.00
	KS	0.05	0.00	0.00	0.00	0.00	0.06	0.00	0.00	0.00	0.00
Floods and ebbs	H	**diff**	**diff**	**diff**	**diff**	**diff**	**diff**	**diff**	**diff**	**same**	**diff**
	P	0.00	0.04	0.00	0.42	0.00	0.00	0.02	0.00	0.38	0.00
	KS	0.22	0.23	0.49	0.20	0.70	0.23	0.25	0.40	0.20	0.70
Flood: Oct and Nov	H	**diff**	**same**	**same**	**same**	**same**	**diff**	**same**	**same**	**same**	**same**
	P	0.00	1.00	1.00	1.00	1.00	0.00	1.00	1.00	1.00	1.00
	KS	0.1	0.00	0.00	0.00	0.00	0.12	0.00	0.00	0.00	0.00
Ebb: Oct and Nov	H	**diff**	**same**	**same**	**same**	**same**	**diff**	**same**	**same**	**same**	**same**
	P	0.00	1.00	1.00	1.00	1.00	0.00	1.00	1.00	1.00	1.00
	KS	0.05	0.00	0.00	0.00	0.00	0.09	0.00	0.00	0.00	0.00

relative to the mean (which will therefore be zero, whilst *δpower* can be negative) see Eq. 2: $\delta power = \frac{\sigma}{\overline{P}} \times 100\%$ [Eq. 2]. Whilst the standard deviation of power within the time-mean window is expressed in units of percentage relative to rated power, the power variability (*δpower*) is important for downscaling resource ocean model information to 0.5 Hz power. All power data was therefore included in the distribution of power variability, including outliers when no power was recorded even above rated speed (see Figs. 2 and 3), because a realistic representation of synthesised power and electricity can therefore be achieved using resource model information.

Turbulence Intensity (TI) was calculated using the 10 min moving mean velocity ($\overline{U}$) and associated standard deviation (σ) of turbulence fluctuations (u') within the moving average window using Eq. 3: $TI = \frac{\sigma}{\overline{U}} \times 100\%$ [Eq. 3]. The major impact of energy variability on power quality is in relation to the deviation of voltage from the rated value – this will be referred to as 'voltage variability' in the paper. Voltage variability (F) was calculated as normalised root mean squared error associated with the running-mean shoreside measured voltage ($\overline{V}$) and associated variability ($V_t - \overline{V}$) of the shoreside measured voltage; see Eq. 4 (where b = a+10 min and n is record length) in line with previous studies of relative voltage change [44,45]: $F = \left(\left(\frac{\sum_{t=a}^{t=b} (V_t - \overline{V})^2}{n} \right) \div \overline{V} \right) \times 100$ [Eq. 4].

4. Results

Using a 10 min moving average on the 0.5 Hz data, the mean tidal current and associated turbulence intensity (Eq. 3), as well as turbine measured power and voltage variability (Eq. 4) was calculated; see Fig. 6 and Fig. 7 for 26-Oct-2014 and 26-Nov-2014 respectively. The Kolmogorov-Smirnov test (KS) for goodness of fit results (Table 1) indicate the data of the two tidal cycles (Oct and Nov) are similar (at 5% significance level), but significant flood/ebb asymmetry is present in both tidal current and turbine power (Figs. 6 and 7). FFT analysis of the 0.5 Hz data (Fig. 4) suggests

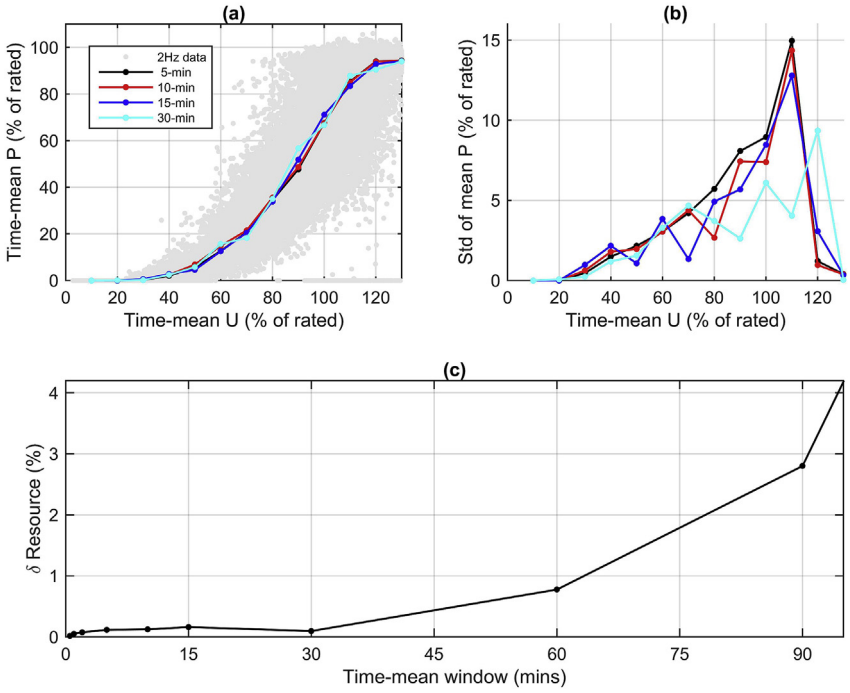

Fig. 5. The observed variability of the 0.5 Hz measured power curve and various time-average windows (panel a). The standard deviation of the associated time-averaged power (P) and velocity (U) is shown in Panel b, and the associated error (as a percentage) in panel c: this shows the reduction in the sum of the power time-series using time-averaged data for the two tidal cycles compared to the 0.5 Hz data.

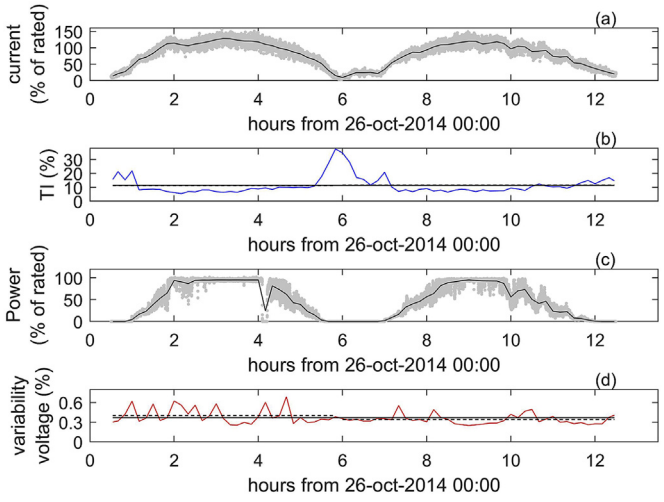

Fig. 6. Tidal-stream power and turbine produced electricity quality for the 26-oct-2014 tidal cycle. The hub-height tidal current speed measured at 0.5 Hz, with the 10 min moving average (black line) is shown in panel a. The associated turbulence intensity (TI) shown as a blue line in panel b, with tidal cycle average as a black line (flood and ebb means are dashed lines, with no disernable difference at this scale). The 0.5 Hz turbine measured power and 10 min mean (black line) is shown in panel c. The shore-side measured voltage variability shown as a red line in panel d, with tidal cycle average as black line, with flood and ebb mean values as dashed line. (For interpretation of the references to colour in this figure legend, the reader is referred to the Web version of this article.)

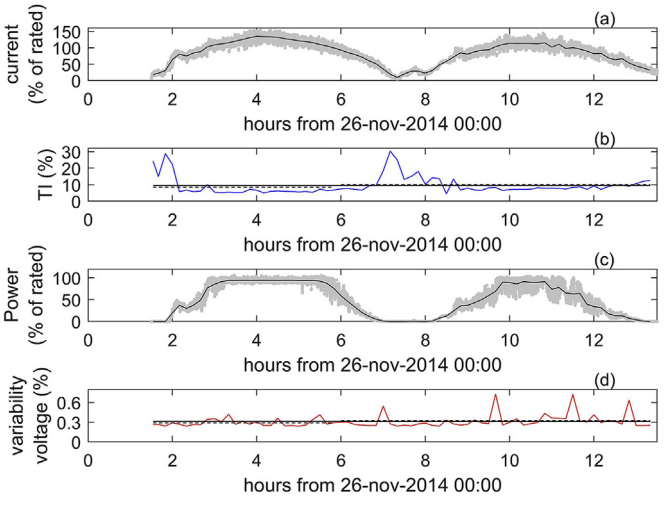

Fig. 7. Tidal-stream power and turbine produced electricity quality for the 26-nov-2014 tidal cycle. The hub-height tidal current speed (panel a) measured at 2 seconds, with the 10 min moving average (black line). The associated turbulence intensity (TI) shown as a blue line in panel b, with tidal cycle average as a black line (flood and ebb means are dashed lines, with no disernable difference at this scale). The 0.5 Hz turbine measured power and 10 min mean (black line) is shown in panel c. The shore-side measured voltage variability shown as a red line in panel d, with tidal cycle average as black line, with flood and ebb mean values as dashed line. (For interpretation of the references to colour in this figure legend, the reader is referred to the Web version of this article.)

varibility in power around ~10 s, potentially due to waves and with slightly higher TI values in October (Fig. 6), the effect is removed with the time-averaging window and hence the similarity test result of Table 1.

In both Figs. 6 and 7 the ebb tide appears first in the time series (the conditions between zero hours and ~6 h). The ebb tidal condition has comparatively larger associated current speeds than the flooding tide in both dates; with larger broad-scale variability features in the flooding tide (see black line of 10-min moving average) and slightly higher turbulence intensity (TI) values, which is shown in Table 2. No strong linear correlation between voltage variability (F), mean flow speed or TI was found ($R^2 < 9\%$), with the

flood and ebb mean F values at ~0.3% (Table 2). A voltage variation below 3% at 1 Hz or 0.3% at 8.8 Hz is defined as "tolerable" [45], which interpolating this to 2 s data suggests a tolerable level of less than 2.4% voltage variation. Furthermore, although some higher F values can be seen in Figs. 6 and 7, all F values are well below that defined as "tolerable".

The hypothesised correlation between current speed variability (defined here as Turbulence Intensity, TI) and the variability in tidal turbine power produced is explored further in Fig. 8, with the linear correlation statistics detailed in Table 3. The strong relationship between mean flow speed, TI and variability of tidal turbine produced power ($\delta power$), within the 10-min running mean, can be clearly seen in Fig. 8d. Power variability ($\delta power$) was found to decrease with increasing mean flow speed (Fig. 8a), largely because it is a percentage of the variability around the mean value and the mean power increases with flow speed. However, the more pronounced effect (based on the flood-ebb distributions in Table 1) of decreasing power variability with increasing flow speed (and decreasing TI) on the ebb tides (gradient, m, of Table 3) appears to drive the significant differences of the fine-scale power variability between the flood and ebb data (R^2 values in Table 3). Further, power variability ($\delta power$) was found to increase with increasing levels of TI, as shown in Fig. 8c and largely because TI decreases with increasing mean flow speeds (Fig. 8b); hence the relationship shown in Fig. 8d and described in Table 3.

A multiple linear regression was performed on the flood and ebb tide grouped data when current speed was above ~30% of rated velocity (called the turbine cut-in speed: the mean speed at which tidal power starts to be produced); giving the variability of power (δ *power*), within the 10 min moving average (as a percentage relative to the mean), with respect to mean flow speed ($\overline{U}$ as a percentage of rated velocity) and TI. The result of the multiple regression is shown in Eqs. (5) and (6), with an associated R^2 of 71% and 77% for flood and ebb tides respectively:

$$\delta power\ (flood) = 34.90 - 0.38\overline{U} + 0.52TI + 0.02(\overline{U} \times TI) \quad (5)$$

$$\delta power\ (ebb) = -42.87 + 0.25\overline{U} + 9.19TI - 0.05(\overline{U} \times TI) \quad (6)$$

Not all variability was captured with a multiple linear regression (Eqs. (5) and (6), and Fig. 8d), potentially due to turbine behaviour and flow characteristics being measured at the turbine hub-height (instead of the entire turbine swept area) - as well as a likely phase lag between observed flow variations and power produced by the turbine. Another method is therefore required to resolve the fine-scale variability to enable synthetic power production models for energy system design. Instead, we explored the distribution of power variability (with respect to the 10-min mean power) to understand how to cascade resource hydrodynamic model information into fine-scale predictions of electricity production. Indeed, bias in the distribution of power variability must be present because there is a clear reduction in the net power over the two tidal cycles when using a running average window on the 0.5 Hz normalised power; as shown in Fig. 5c.

The variability of power relative to the 10-min mean (δP) and the distribution of power varibility within the 10-min running mean of the 2 s data is shown in Fig. 9. The distribution of the fine-scale variability of power clearly becomes more leptokurtic (sharply peaked) with increasing flow speeds in Fig. 9; for both flood and ebb tidal conditions the power fluctuations become less compared to the mean. However, the shape of the distribution in power variability appears to change in Fig. 9, which is important to understand for bias correction in resource assessment (e.g. see Fig. 5c). Characterisation of the relative power variability distribution will allow a synthetic power production model to be used to represent fine-scale tidal power variability; hence hydrodynamic resource model output (typical outputs of 30–60 min) could be downscaled to predicted power at 0.5 Hz (of potential use to system operators).

The distribution of tidal velocity and tidal turbine power in Fig. 10 shows interesting trends when grouped (data grouped between flood and ebb tides – and for tidal current speeds): below turbine cut-in speed (i.e. U is ~30% of rated U), between cut-in and rated velocity, and above rated velocity. Velocity variance, relative to the time-averaged 10-min mean ($\overline{x}$) (Fig. 10a and b), was normally distributed, matching a normalised Gaussian distribution described by Eq. 7 (where σ is standard deviation): $y = \frac{1}{\sigma\sqrt{2\pi}} e^{-\frac{x-\overline{x}}{2\sigma^2}}$ [Eq. 7]. The power variability (relative to the 10-min mean power) is not normally distributed (see Fig. 10 and Table 4); hence, there is an over-estimation of energy if we do not include the effects of turbulent fluctuation on power (see Fig. 5c) and the discretised distribution of fine-scale power variability (see Fig. 9). The negatively skewed (S) distribution of the power variability is shown in Fig. 11 and Table 4, alongside the Kurtosis (K) of the distribution.

Fig. 11 shows how the variability (e.g. standard deviation, σ in Fig. 11b) of normalised power increases with tidal current speed (U), becoming more negatively skewed (Fig. 11c) with increasing Kurtosis values (Fig. 11d); indicating normalised power variability distributions are asymmetric, with heavier distribution-tails and sharper peaks as velocity increases – especially pronounced in Ebbing tide data (shown in Fig. 10) when voltage variability (F) is slightly higher and yet the turbulence intensity is lower (Figs. 7 and 8). The result of the power variability distributions in Table 4 (using the Lilliefors test, with a hypothesis the data is from a normal distributed at the 5% significance level), Kurtosis and Skew results for discretised velocity groups, alongside the parameters of the best fitting distribution, found fine-scale power variability to best described by the *t location scale* distribution; where distributed velocity groups (x) in a probability distribution (y) is described in Eq. (8), with the gamma function (Γ) and parameters of shape (υ), scale (ϑ) and location (μ); shown in Table 4 (as these parameters, which describe the distribution's shape, vary with current speed):

$$y = \frac{\Gamma\left(\frac{\upsilon+1}{2}\right)}{\sqrt{\upsilon\pi}\,\Gamma\left(\frac{\upsilon}{2}\right)} \left[\frac{\upsilon + \left(\frac{x-\mu}{\vartheta}\right)^2}{\upsilon}\right]^{-\left(\frac{\upsilon+1}{2}\right)} \quad (8)$$

Applying this *t location scale* distribution (Eq. (8)), with the shape (υ), scale (ϑ) and location (μ) parameters (shown in Table 4, and Fig. 12 for finer discretisation of velocity groups, i.e. 10% U groups), allows synthetic power to be generated using low temporal resolution velocity data. Therefore, a fine-scale tidal-stream turbine power time-series can be generated using low resolution

Table 2
Mean values of variability associated with two tidal cycles of tidal-stream turbine data, also split into flooding and ebbing tides: voltage variability, calculated using the varibility of 0.5 Hz measured voltage within a 10-min running mean (Eq. 4), and TI, calculated using varibility within a 10-min running mean of the 0.5 Hz flow speed measured at hub height (Eq. 3).

	voltage variability (F)		Turbulence Intensity (TI)	
	flood	ebb	flood	Ebb
26-Oct-14	0.31%	0.33%	11.7%	11.3%
26-Oct-14	0.29%	0.33%	9.7%	9.4%

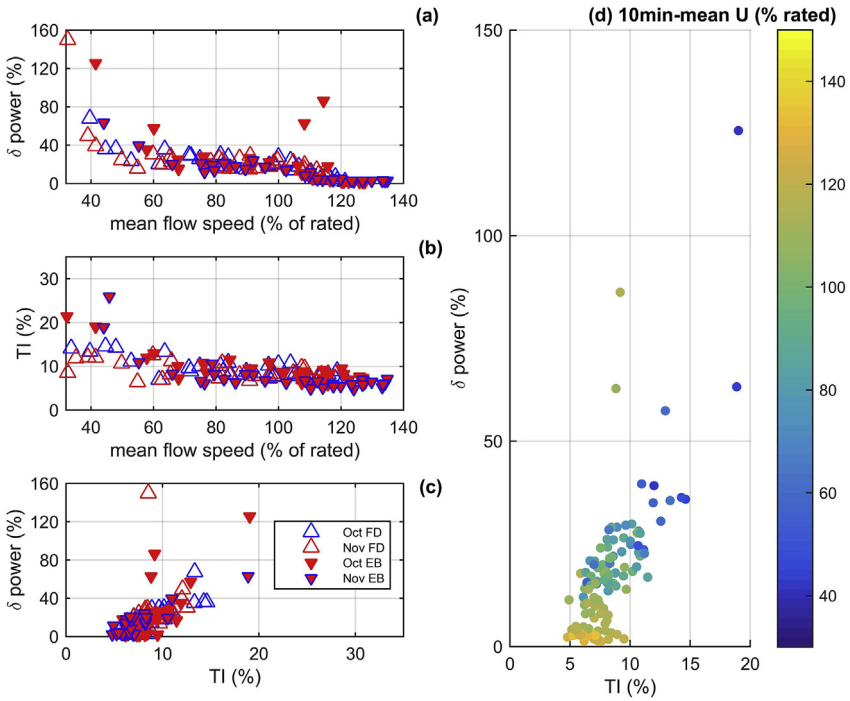

Fig. 8. The relationship between 10-min averaged tidal-stream turbine data and grouped by date (26-Oct-14 and 26-Nov-14) and flood (FD) or ebb (EB) tidal condition (see legend). Mean flow speed and 10-min tidal turbine power variability (***δ power*** calculated from Eq. 2) shown in panel a; mean flow speed and Turbulence Intensity (TI calculated from Eq. 3) shown in panel b; power variability (***δ power***) and TI shown in panel c. All 10-min data is shown in panel d as the relationship between power variability and TI, with mean flow speed shown as colours. (For interpretation of the references to colour in this figure legend, the reader is referred to the Web version of this article.)

Table 3
The linear regression data between 10-min mean flow speed ($\overline{U}$), Turbulence Intensity (TI calculated from Eq. 3) and 10-min tidal turbine power variability (***δ power*** calculated from Eq. 2), for the tidal-stream turbine power quality data described in Fig. 7; when flow speed >35% rated. The gradient (m) and intercept (c) of the linear regression within form $y = mx+c$ with associated R^2 value, and data grouped by date and tidal stage (flooding or ebbing tidal condition).

Data tested	Grouped data	Gradient (m)	Intercept (c)	R^2 (%)
δ power (y as %) and $\overline{U}$ (x as % rated) (Fig. 8a)	floods Oct	−2.24	258	35
	flood Nov	−0.78	96	48
	ebbs Oct	−0.46	62	71
	ebbs Nov	−0.63	78	39
	Floods	**−0.39**	**55**	**63**
	Ebbs	**−0.75**	**95**	**43**
TI (y) and $\overline{U}$ (x) (Fig. 8b)	floods Oct	−0.07	16	62
	flood Nov	−0.04	12	35
	ebbs Oct	−0.11	20	67
	ebbs Nov	−0.11	19	49
	Floods	**−0.05**	**14**	**43**
	Ebbs	**−0.10**	**19**	**50**
δ power (y) and TI (x) (Fig. 8c)	floods Oct	30.87	−257	51
	flood Nov	3.68	−7	6
	ebbs Oct	22.77	−173	63
	ebbs Nov	6.66	−34	90
	Floods	**4.17**	**−17**	**54**
	Ebbs	**6.98**	**−38**	**75**

tidal current data (i.e. from a hydrodynamic resource model), which can be used for electrical system and grid integration analysis. To demonstrate this synthetic power production model, a realistic fine-scale tidal power time-series (at 2 s) was generated using tidal velocity data output from a hydrodynamic tidal-resource model (of [37]) at a frequency of 30 min, and the idealised power curve presented by Lewis et al. [10] - see Fig. 3.

The synthesised fine-scale power model is compared to that measured for the 26-Nov-2014 data in Fig. 13. Although the 30 min hydrodynamic model tidal velocity data has none of the characteristics of the tidal-stream energy device (apart from cut-in and rated power values; see Fig. 3), the distribution of fine-scale power are similar; as shown in the "QQ" (quantile-quantile) plot of Fig. 13d, which shows the two distributions are similar (at the 5% significance level) with a KS test result of 0.03 (P value < 0.01). Therefore, using a synthetic power production model (using *t location scale* distribution, with the shape (υ), scale (ϑ) and location (φ) parameters of Table 4, and in Fig. 12), fine-scale realistic power can be predicted at 0.5 Hz based on 30 min velocity data; an important step for grid-integration within electrical systems.

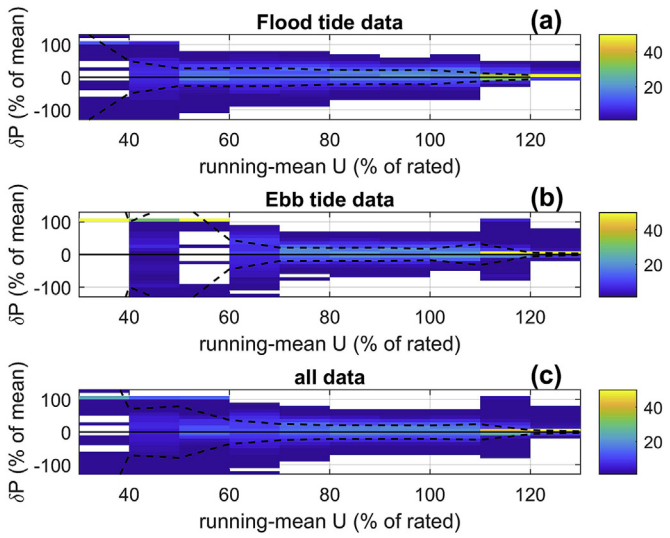

Fig. 9. The probability distribution (coloured scale) of the relative (compared to the mean) variability of tidal-turbine power (δP), within a 10-min moving average, compared to the flow speed, for the tidal turbine data of the 26-Oct-14 and 26-Nov-14 and grouped into flood (a) and ebb (b) and all (c) tidal conditions.

5. Discussion

Rapid fluctuations in power generated by renewable energy sources are known to cause problems to power system operation because they result in power unbalance and power quality issues [46]. Fine-scale variability of power from a tidal-stream turbine was observed for a site in Orkney (Fig. 3). This variability is shown to have a bias, because there is a reduction in the net power in two tidal cycles when the averaging period is increased (Fig. 5c). However, fine-scale power variability had only a small effect on resource estimates (Fig. 5), with less than 1% error in the energy harvested by the tidal turbine for frequencies typical of resource modelling studies. Hence, a standardised device power curve can be applied to coarse hydrodynamic resource model data for accurate resource assessment without the need to include fine-scale resource variability (i.e. turbulence) or device characteristics (beyond swept area, cut-in and rated speed and power). Furthermore, fine-scale power variability (see Fig. 3) can be statistically characterized, and downscaled, for electricity supply design strategies (Fig. 13). Therefore, this study provides the first discussion of the power and electricity being produced by tidal-stream turbines.

A strong linear relationship was found between power variability, associated with a 10 min running mean, and both turbulence intensity and mean flow speed (see Table 2). Power fine-scale varibility characteristics were consistent for a wide range of time-averaging windows (Table 1), but there were clear differences between the flooding and ebbing tide data. For example, by applying the multi-regressional result in Eq. (5) (flooding) and Eq. (6) (ebbing), fine-scale rotor-power varibility was estimated to be ±20% (flood tide) and ±24% (ebb tide) for the tidal-stream turbine operating in a 2.5 m/s mean flow with a Turbulence Intensity of 10%. Although very few studies exist, for the two dates when tidal power was measured (Table 1), the observed fine-scale power variability was similar to that measured in other tidal turbines at different locations (e.g. Refs. [45,47]). Our observations of fine-scale turbine power variability were higher than those measured in a lower turbulence environment [45,48], yet average TI values measured in our study were lower than those measured at another tidal-stream energy site [23,25]: 9–12% compared to 12–13%.

Flood-ebb asymmetry was found in our study, with faster ebb current speeds and higher turbulence measurements (mean TI of

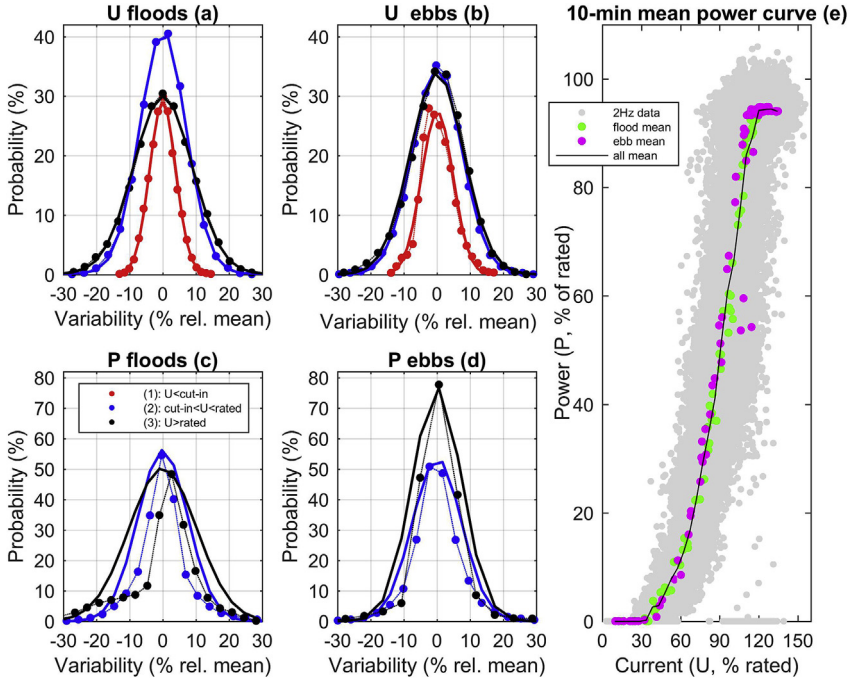

Fig. 10. The probability distributions of the 10-min running mean data grouped by flow seed conditions: (1) flow speeds less than cut-in speed of turbine (U<30% of rated speed); (2) flow speeds between cut-in and turbine rated speed (cut-in<U<100%); (3) flow speeds greater than turbine rated speed; shown as red, blue and black lines respectively with thin dashed lines connecting data points (circles) with the respective normal distribution (normalised) shown as thicker solid line. Flooding tide flow speed (panel a) and ebb tide flow speed (panel b) distributions are shown with respective turbine power distributions (panel c and d respectively), with the 10-min running mean power curve show in panel e. (For interpretation of the references to colour in this figure legend, the reader is referred to the Web version of this article.)

Table 4
The 10-min probability distribution information of 0.5 Hz normalised tidal turbine power variability for two tidal cycles, and also grouped by tidal current speed, with velocity (U) below turbine cut-in speed (U<30% of rated velocity, when no power is produced), U between cut-in (30%) and rated turbine velocity (100%), and when current speeds are above rated velocity of the turbine (U>100%). The distribution that closest matches that observed is described and the KStest result given (with associated P-value), and the parameters required to describe this distribution given.

Grouped data result (based on velocity		Velocity (U)			Power (P)	
		U<30%	30%<U<100%	U>100%	30%<U<100%	U>100%
Flooding tide	Mean ($\bar{x}$)	−0.05	0.00	0.00	0.00	0.00
	S.D. (standard deviation, σ)	3.96	6.95	8.86	7.56	10.22
	Kurtosis (K)	3.09	3.43	3.12	6.07	4.16
	Skewness (S)	0.11	−0.10	−0.09	0.58	−0.90
	KStest result and p-value (in brackets)	0.01 (0.07)	0.01 (0.01)	0.01 (0.02)	0.11 (0.00)	0.16 (0.00)
	Closest distribution:	**normal**	**normal**	**normal**	**T-location**	**T-location**
	location (μ)	n/a	n/a	n/a	−0.26	2.09
	scale (ϑ)	n/a	n/a	n/a	4.01	5.34
	shape (υ)	n/a	n/a	n/a	2.04	1.86
Ebbing tide	Mean ($\bar{x}$)	0.09	0.00	0.00	0.00	0.00
	S.D. (standard deviation, σ)	4.78	7.47	8.08	7.44	11.67
	Kurtosis (K)	3.41	3.53	3.46	5.41	14.87
	Skewness (S)	0.29	−0.07	−0.29	0.17	−1.58
	KStest result and p-value (in brackets)	0.04 (0.00)	0.02 (0.00)	0.02 (0.00)	0.07 (0.00)	0.24 (0.00)
	Closest distribution:	**normal**	**normal**	**normal**	**T-location**	**T-location**
	location (μ)	n/a	n/a	n/a	−0.18	0.30
	scale (ϑ)	n/a	n/a	n/a	5.01	2.29
	shape (υ)	n/a	n/a	n/a	3.18	1.14

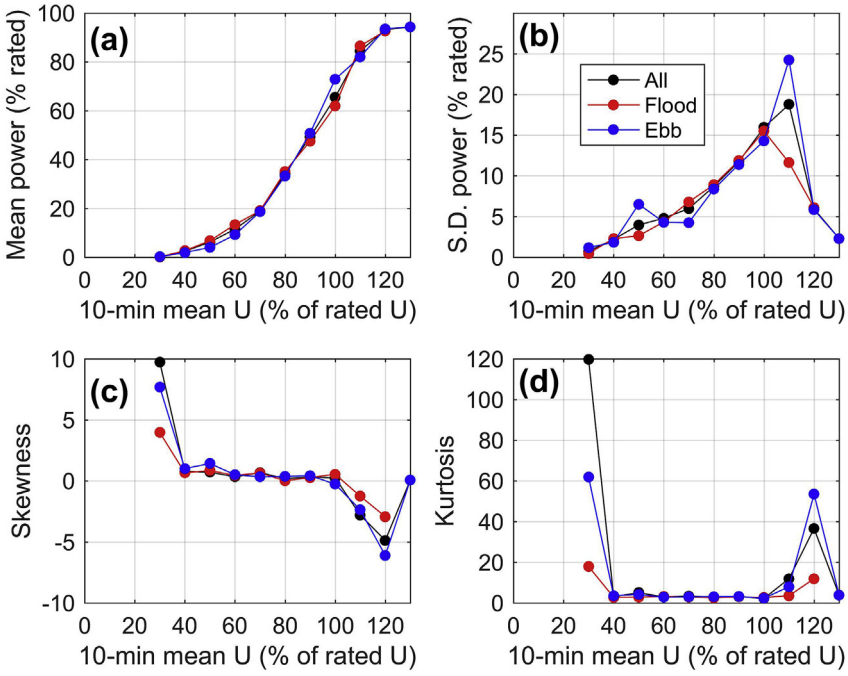

Fig. 11. The variability associated with the normalised 10-min moving window power average, measured at 0.5 Hz from a tidal turbine for two tidal cycles. The 10-min mean power curve for all data, and grouped into flooding and ebbing tides (panel a), with the standard deviation (S.D.), Skewness and Kurtosis of the power variability distributions in panels b, c and d respectively; and discretised to the nearest 10% velocity (U) group.

~9% during the ebb and 12% during the flood; Table 2), matching those simulated in the Fall of Warness [37]; and other sites (e.g. Refs. [23,25]). Fine-scale power variability was higher during the flood tide, likely because current speeds are lower then and power variability decreased with high current speeds (above rated velocity, when power capping also occurred; see Figs. 9–11). Moreover, an oscillation in the mean current speed and power during the flooding tide was observed for both dates (Figs. 6 and 7), which may also explain the increase in flood-tide power variability. This broad-scale oscillation feature of the flood tide was not predicted by the [37] model, but could be caused by an eddy feature (perhaps generated by a neighboring bathymetric or topographic feature and then migrating through the site as it is sheds and persists [49]). This variability in flow direction may be the cause of some recorded power variability, and future work ought to resolve current direction as well as magnitude. For example, zero power was recorded for some instances of high current speeds (Figs. 2C and 3), which may be due to changes in tidal current direction causing turbine blade stall, although this event occurred during a period of large waves and thus could be due to wave-tide interaction processes [50].

The Fast Fourier Transform (FFT) of tidal turbine power (Fig. 4)

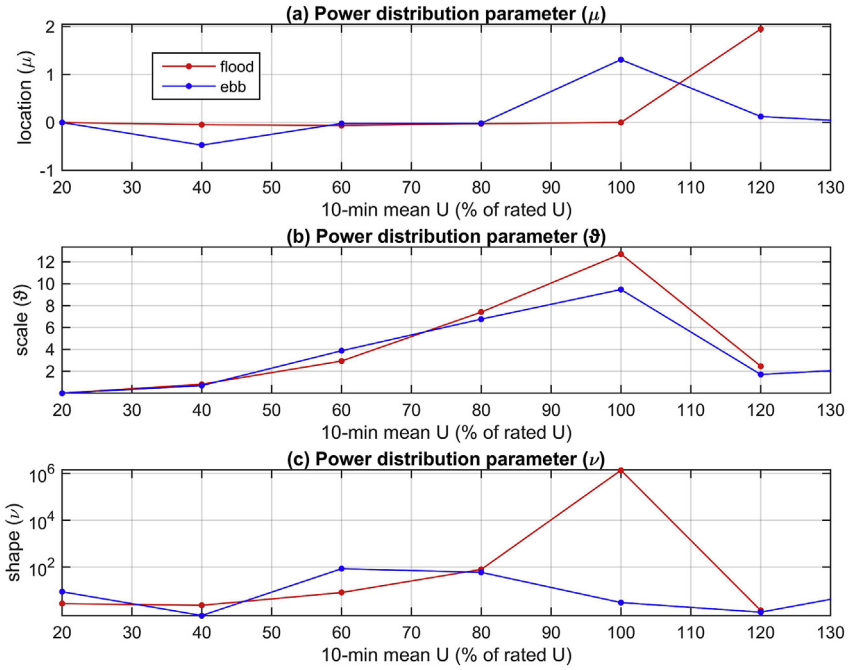

Fig. 12. The three parameters used to describe the t-location scale distribution of 0.5 Hz power, when using a 10-min moving average and normalising the power by rated velocity and the variability around the mean – grouped by flood and ebb tide for two tidal cycles (26-Nov and 26-Oct 2014), with data normalised by rated velocity and power.

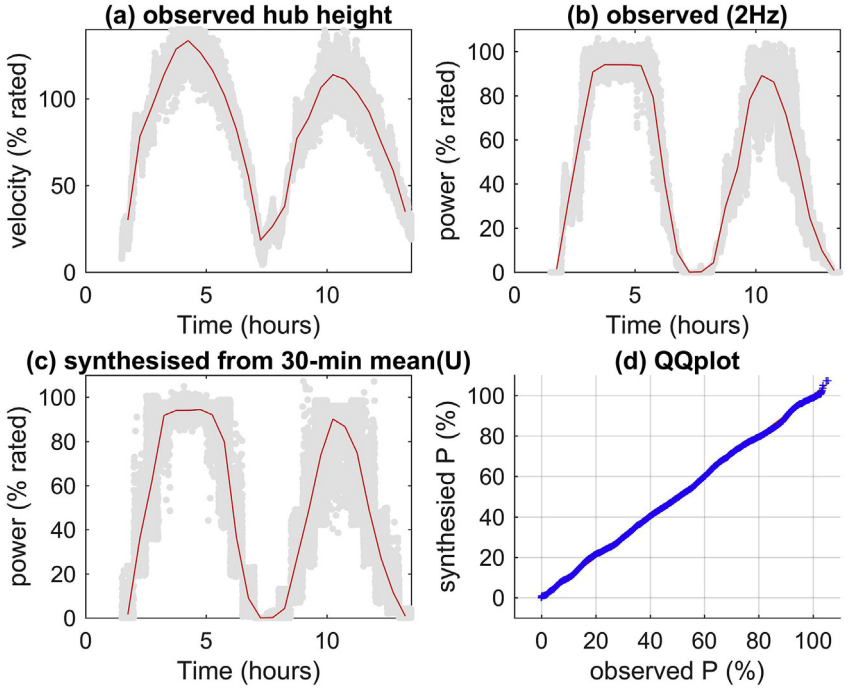

Fig. 13. The synthetic fine-scale power produced from a tidal turbine. The 0.5 Hz observed (grey shaded) and 30min frequency hydrodynamic model predicted (red line) hub-height tidal current speed in panel a, with the observed 2 Hz tidal-turbine power in panel b (with red line a 30-min moving average). Panel c shows the 30-min hydrodynamic resource model power time-series (calculated using idealised power curve of Fig. 2) and the synthesised 0.5 Hz power (grey; calculated applying the *t-location scale* distribution parameters of Fig. 11), with the similarity of the 0.5 Hz synthesised power (P) and that observed (P) in panel d. (For interpretation of the references to colour in this figure legend, the reader is referred to the Web version of this article.)

produced similar results to those by Thiringer et al. [48]; with two exceptions: Firstly, the spectral peak associated with a ~10 s period, in both power (Fig. 4a) and hub height current speed (Fig. 4c) for the October data. Secondly, the temporal resolution of the power measurements in this study were not high enough to resolve the modes of power oscillation observed by Thiringer et al. [48] below 2 s, which were potentially due to the turbine blade passing the support structure [51]. The spectral peak within the October data coincided with a large wave event offshore of the site (based on ERA-interim data the 0.125° resolution re-analysis product; see

Ref. [42]), and could be scope for future research as waves are known to affect the tidal resource [50] and measurements of turbulence [24]. Indeed, the results of our power quality analysis may be considered location and device-specific (e.g. rotor speed control mechanisms, such as pitch control, may differ between devices; [52]). Further work is needed to assess the quality of tidal-stream electricity at a variety of sites in comparison to other forms of renewable energy. Further work is also needed to understand the effect of fine-scale tidal turbine power variability when aggregated to the power output from an array of devices (see Ref. [45]). For example, variability in wave energy is well known but can be mitigated by a number of spatially separated sites [53].

The estimated tidal turbine voltage variability (F) matches that measured by MacEnri et al. [45] for the SeaGen tidal device, with values within the limit defined as tolerable (no strong linear correlation between F, mean flow speed or TI was found, and mean F values were ~0.3%); especially considering the relative large contribution of a 1 MW turbine to the Orkney grid (~5 MW). Therefore, tidal energy voltage and power variability is less severe than reported in other forms of renewable energy [54,55]. Although further work is needed to fully assess the impact of tidal energy on power quality, tidal energy is likely to be more dispatchable than other renewable sources due to the higher predictability.

The power variability observed in this study agrees with [29], who report the variability of tidal energy to be much better than other forms of renewable energy, such as wind (e.g. Ref. [56]) and wave energy (e.g. Refs. [54,55]). Indeed, storage mechanisms to mitigate the effects of renewable power variability (such as flywheel and batteries; e.g. [57]), can also be applied to tidal energy; for example, as tidal energy is surrounded by water, novel pumped-hydro [57] and hydrogen [58] storage solutions could be incorporated.

The characterisation of tidal power variability, for storage solution design and optimization, is clearly an important research question that future studies should aim to resolve (e.g. the size of storage required for electricity users may not be large in comparison to other renewable forms). Indeed, tidal energy is considered one of the more expensive renewable electricity forms [59], and energy storage would increase costs further. Therefore tidal energy integration may appear less expensive when the costs of both technologies are included (i.e. Levelised Cost of Energy, storage and grid integration solutions) – especially within micro-grids with a high penetration of intermittent and less controllable renewable energy forms (for example, 100% renewable energy micro-grids for remote communities in fuel poverty).

Another method to mitigate the impact of fluctuations in renewable power supplied to the power grid, as well as design effective system control measures, is to accurately predict power variability. Methods of predicting power variability are well established in the wind industry, by using high-fidelity and computationally expensive Large Eddy Simulation (LES) models to simulate fine-scale wind field progression through a site, and thus predict fluctuations within the wind resource (e.g. Ref. [60]). Tidal energy is often stated to be predictable, due to the periodicity of the tide [18], yet predictions of turbulent fluctuations in the tidal current would require similar LES methods. Another method of predicting fluctuations in the tidal energy resource could be established with a power variability probability density distribution, as has also been applied in the wind industry [46].

In our study, tidal velocity characteristics did not fully, and directly, characterize the observed power variability (Table 2) – potentially as velocity measurements made at hub height cannot represent flow characteristics throughout the entire turbine swept area. Therefore not all variability observed in Fig. 3 can be quantified due to instrument uncertainty and the lack of high-resolution flow data throughout the swept area of the turbine, which should be investigated in future studies; however the observed variability of measured power can be statistically characterized (Fig. 10). Fine-scale power variability distributions enable a simple statistical prediction method for energy supplied by a wind turbine based on synoptic (i.e. mean flow) information (e.g. Refs. [57,58], noted as computationally less expensive [46], and allow comparisons of power quality to be made between wind and tidal turbines).

The tidal turbine power variability (shown in Figs. 9 and 10) was found to be different to that of wind turbines. This variability can also clearly be seen in Fig. 3, and the analysis of power variability in Fig. 10 (~60%) finds the distribution is similar to that shown by Ren et al. [58]; but only the resource (current speed variability), not power, matched a Gaussian distribution found by Ren et al. [58]. Further, the Weibull or Rayleigh distributions of power reported by other authors [57,61] were not found in this study. Furthermore, wind power variability estimates appear to be an order of magnitude greater than observed in our tidal turbine data, due to the Weibull or Rayleigh distributions [57,61].

Fine-scale tidal turbine power variability was found to be well described by the *t location scale* distribution; where distributed velocity groups (x) in a probability distribution (y) are described in Eq. (8), with the gamma function (Γ) and parameters of shape (υ), scale (ϑ) and location (μ); shown in Table 4. Therefore, the likely tidal power at 0.5 Hz can now be predicted based on 30-min-averaged current speeds output from an ocean model (or using a tidal prediction algorithm), together with knowledge of cut-in and rated velocity of the tidal turbine (the idealised power curve of [10] assumes a device efficiency, *Cp*, of 60% within Equation 1).

When using the 30-min hydrodynamic model simulations of [37] and an idealised power curve of Lewis et al. [10]; the fine-scale power variability model performed well (R^2 85% and RMSE of 14%, but with an energy difference of less than 0.7% for the tidal cycle), and produced a statistically similar distribution (see Fig. 13) of power variability. Therefore, the variability observed in Fig. 3 can be resolved, and coarse hydrodynamic resource model data can be statistically downscaled to provide accurate resource predictions, even at very high temporal resolution and with a idealised power curve based on a different tidal turbine (twin rotor MCT device – see Ref. [10]). Considering the current high cost of tidal-stream energy, compared to other temporal variability renewable energy sources, the predictability of tidal-stream energy could be an asset in high penetration renewable energy distributed electricity supplies.

Future work could improve on the simple statistical model presented here (downscaling resource to 0.5 Hz power), by increasing the observational data and the dependency of fine-scale turbulent fluctuations (i.e. the temporal clustering of power variability). In the sampling of the statistical distribution, to downscale hydrodynamic model 30-min data to 2 s power production, independence between data was assumed (i.e. a turbulent fluctuation synthesised at time t will not influence the next iteration at time $t+\delta t$). Future work should also aim to validate this fine-scale power prediction tool for different devices and sites, as well as exploring the use of power supply prediction in micro and national-scale grids to determine the true value of tidal power within a future renewable energy mix.

6. Conclusion

The temporal variability and predictability of tidal-stream power was measured from a grid-connected 1 MW turbine in a highly energetic tidal site. Voltage variability was well within tolerable limits and no significant effect to estimates of annual mean energy

yield were found (i.e. 1% reduction in energy calculated for typical resource assessment frequencies). Therefore, resource uncertainty due to fine-scale power variability appears low for tidal-stream energy, and idealised power curves (with accurate cut-in and rated flow speeds) are suitable for resource assessments – which we show can be statistically downscaled to fine-scale (2 Hz) power prediction. The value of tidal energy in power systems therefore appears to be undervalued, since this resource is perceived as being expensive (e.g. Levelized Cost Of Energy), without accounting for predictability. A skillful, yet simple, probability distribution model of power variability was applied to 30-min hydrodynamic model data (tidal velocity at hub height) using the *t location scale* distribution, with parameters based on mean flow speed (which also described turbulence characteristics). Therefore, synthetic turbulence and fine-scale tidal turbine power variability model can be applied to low-temporal resolution resource data, with an idealised power curve, for a computationally efficient prediction of tidal-stream power.

Acknowledgements

This paper was the result of a collaboration funded by the Welsh Government and Higher Education Funding Council for Wales through the Sêr Cymru National Research Network for Low Carbon, Energy and Environment. SPN and MJL wish to acknowledge the support the Sêr Cymru National Research Network for Low Carbon, Energy and the Environment (NRN-LCEE) and the EPSRC METRIC project EP/R034664/1. The authors also wish to thank Dr. Phil Coker from Reading University, UK for his useful comments and discussion. AGB wishes to acknowledge the financial support of the Welsh European Funding Office, and the European Regional Development Fund Convergence Programme.

Appendix A. Supplementary data

Data in this publication was allowed through a NDA and so is not publically accessible data. However, the hydrodynamic models and standardised method, applied throughout the publication, will allow replicability (because percentage change analysis was applied). Therefore, supplementary data to this article can be found online at https://doi.org/10.1016/j.energy.2019.06.181. Further details of the data are given in McNaughton [38] and Ahmed et al. [39]. Furthermore, data are available via the University of Edinburgh's data share (http://redapt.eng.ed.ac.uk).

References

[1] Drew DR, Coker PJ, Bloomfield HC, Brayshaw DJ, Barlow JF, Richards A. Sunny windy sundays. Renew Energy 2019;138:870–5.
[2] Barton JP, Infield DG. Energy storage and its use with intermittent renewable energy. IEEE Trans Energy Convers 2004;19(2):441–8.
[3] Joos M, Staffell I. Short-term integration costs of variable renewable energy: Wind curtailment and balancing in Britain and Germany. Renew Sustain Energy Rev 2018;86:45–65.
[4] Carrasco JM, Franquelo LG, Bialasiewicz JT, Galván E, PortilloGuisado RC, Prats MM, León JI, Moreno-Alfonso N. Power-electronic systems for the grid integration of renewable energy sources: A survey. IEEE Trans Ind Electron 2006;53(4):1002–16.
[5] Liserre M, Sauter T, Hung JY. Future energy systems: Integrating renewable energy sources into the smart power grid through industrial electronics. IEEE Ind Electron Mag 2010;4(1):18–37.
[6] Milan P, Wachter M, Peinke J. Stochastic modelling and performance monitoring of wind farm power production. J Renew Sustain Energy 2014;6:033119.
[7] Brouwer AS, Van Den Broek M, Seebregts A, Faaij A. Impacts of large-scale Intermittent Renewable Energy Sources on electricity systems, and how these can be modeled. Renew Sustain Energy Rev 2014;33:443–66.
[8] Wan C, Zhao J, Song Y, Xu Z, Lin J, Hu Z. Photovoltaic and solar power forecasting for smart grid energy management. CSEE J Power Energy Syst 2015;1(4):38–46.
[9] Sun T, Wang WS, Dai HZ, Yang YH. Voltage fluctuation and flicker caused by wind power generation [J]. Power Syst Technol 2003;12:014.
[10] Lewis M, Neill SP, Robins PE, Hashemi MR. Resource assessment for future generations of tidal-stream energy arrays. Energy 2015;83:403–15.
[11] Neill SP, Hashemi MR, Lewis MJ. Optimal phasing of the European tidal stream resource using the greedy algorithm with penalty function. Energy 2014;73:997–1006.
[12] POSTnote. Intermittent electricity generation 2014;464.
[13] Grotz C. The new Germany Renewable Energy Sources Act (EEG) and its impact on wind energy. German Wind Energy Association (BWE) November; 2008.
[14] Pinson P, Mitridati L, Ordoudis C, Ostergaard J. Towards fully renewable energy systems: Experience and trends in Denmark. CSEE J Power Energy Syst 2017;3(1):26–35.
[15] Swain P, Jagadish S, Mahesh KU. July. Integration of renewable sources of energy into power grid. In: 2017 IEEE region 10 Symposium (TENSYMP). IEEE; 2017. p. 1–5.
[16] Albadi MH, El-Saadany EF. Overview of wind power intermittency impacts on power systems. Electr Power Syst Res 2010;80:627–32.
[17] Slootweg JG, Haan SWH, Polinder H, Kling WL. General model for representing variable speed wind turbines in power system dynamics simulations. IEEE Trans Power Syst 2003;18(1):144–51.
[18] Lewis M, Neill SP, Robins P, Hashemi MR, Ward S. Characteristics of the velocity profile at tidal-stream energy sites. Renew Energy 2017;114:258–72.
[19] Hardisty J. Power intermittency, redundancy and tidal phasing around the United Kingdom. Geogr J 2008;174(1):76–84.
[20] Neill SP, Cooper MM, Lewis MJ. Global tidal phasing potential. New Orleans: 2016 Ocean Sciences Meeting; 2016b. p. 21–6. February 2016.
[21] Neill SP, Hashemi MR, Lewis MJ. Tidal energy leasing and tidal phasing. Renew Energy 2016;85:580–7.
[22] Thomson J, Polagye B, Durgesh V, Richmond M. Measurements of turbulence at two tidal energy sites in Puget Sound, WA. IEEE J Ocean Eng 2012;37:363–73.
[23] Milne IA, Sharma RN, Flay RGJ, Bickerton S. Characteristics of the turbulence in the flow at a tidal stream power site. Phil. Trans. Roy. Soc. A. 2013;371:20120196.
[24] Togneri M, Lewis M, Neill S, Masters I. Comparison of ADCP observations and 3D model simulations of turbulence at a tidal energy site. Renew Energy 2017;vol. 114:273–82.
[25] Togneri M, Masters I. Micrositing variability and mean flow scaling for marine turbulence in Ramsey Sound. J Ocean Eng Mar Energy 2015 (2015).
[26] Afgan I, McNaughton J, Rolfo S, Apsley DD, Stallard T, Stansby P. Turbulent flow and loading on a tidal stream turbine by LES and RANS. Int J Heat Fluid Flow 2013;43:96–108.
[27] Blackmore T, Myers LE, Bahaj AS. Effects of turbulence on tidal turbines: Implications to performance, blade loads and conditions monitoring. Int J Mar Energy 2016;14:1–26.
[28] Nishino T, Willden RH. Effects of 3-D channel blockage and turbulent wake mixing on the limit of power extraction by tidal turbines. Int J Heat Fluid Flow 2012;37:123–35.
[29] Magagna D, Uihlein A. Ocean energy development in Europe: Current status and future perspectives. Int J Mar Energy 2015;11:84–104.
[30] Barthelmie R, Hansen O, Enevoldsen K, Højstrup J, Larsen S, Frandsen S, Pryor S, Motta M, Sanderhoff P. Ten years of meteorological measurements for offshore wind farms. J Sol Energy Eng 2005;127:170–6.
[31] Barthelmie RJ, Frandsen ST, Nielsen MN, Pryor SC, Rethore PE, Jørgensen HE. Modelling and measurements of power losses and turbulence intensity in wind turbine wakes at Middelgrunden offshore wind farm. Wind Energy: An Int J Prog Appl Wind Power Convers Technol 2007;10(6):517–28.
[32] Brown AJG, Neill SP, Lewis MJ. The influence of wind gustiness on estimating the wave power resource. Int J Mar Energy 2013;3:e1–10.
[33] Burton T, Jenkins N, Sharpe D, Bossanyi E. Wind energy handbook. John Wiley & Sons; 2011.
[34] Hay AE. Remote acoustic turbulence measurement in a high flow tidal channelvols. 20–22. 2018 Australian Ocean Renewable Energy Symposium; 2018. Nov. 2018.
[35] Hay AE, McMillan J, Cheel R, Schillinger D. September. Turbulence and drag in a high Reynolds number tidal passage targetted for in-stream tidal power. In: Oceans-san Diego, 2013. IEEE; 2013. p. 1–10.
[36] Goward Brown AJ, Neill SP, Lewis MJ. Tidal energy extraction in three-dimensional ocean models. Renew Energy 2017;114:244–57.
[37] Neill SP, Hashemi MR, Lewis MJ. The role of tidal asymmetry in characterizing the tidal energy resource of Orkney. Renew Energy 2014b;68:337–50. Aug 1.
[38] McNaughton J. Tidal turbine wake analysis using vessel and seabed mounted ADCPS. In: Presented at the Oxford Tidal Energy Workshop March 2015; 2015.
[39] Ahmed U, Apsley DD, Afgan I, Stallard T, Stansby PK. Fluctuating loads on a tidal turbine due to velocity shear and turbulence: Comparison of CFD with field data. Renew Energy 2017;112:235–46.
[40] Sellar BG, Sutherland DRJ. Technical report on tidal site Characterisation during the ReDAPT project v4.0, 2016. Institute for Energy Systems, School of Engineering, University of Edinburgh; 2016.
[41] Lewis MJ, Palmer T, Hashemi R, Robins P, Saulter A, Brown J, Lewis H, Neill S. Wave-tide interaction modulates nearshore wave height. Ocean Dynam 2019;69(3):367–84.
[42] Dee DP, Uppala SM, Simmons AJ, Berrisford P, Poli P, Kobayashi S, Andrae U,

Balmaseda MA, Balsamo G, Bauer DP, Bechtold P. The ERA-Interim reanalysis: Configuration and performance of the data assimilation system. Q J R Meteorol Soc 2011;137(656):553–97.
[43] Massey FJ. The Kolmogorov-smirnov test for goodness of fit. J Am Stat Assoc 1951;46(No. 253):68–78.
[44] Larsson A. Flicker Emission of wind turbines during continuous operation. IEEE Trans Energy Convers 2002;17(1):114–8.
[45] MacEnri J, Reed M, Thiringer T. Influence of tidal parameters on SeaGen flicker performance. Phil. Trans. Roy. Soc. A. 2013;371:20120247.
[46] Ellis N, Davy R, Troccoli A. Predicting wind power variability events using different statistical methods driven by regional atmospheric model output. Wind Energy 2015;18(9):1611–28.
[47] Khan J, Bhuyan G, Moshref A, Morison K, Pease JH, Gurney J. July. Ocean wave and tidal current conversion technologies and their interaction with electrical networks. In: Power and energy Society general Meeting-Conversion and Delivery of electrical energy in the 21st Century, 2008. IEEE; 2008. p. 1–8 [IEEE].
[48] Thiringer T, MacEnri J, Reed M. Flicker evaluation of the SeaGen tidal power plant. IEEE Trans Sustain Energy 2011;2(4):414–22.
[49] Neill SP, Jordan JR, Couch SJ. Impact of tidal energy converter (TEC) arrays on the dynamics of headland sand banks. Renew Energy 2012;37(1):387–97.
[50] Lewis MJ, Neill SP, Hashemi MR, Reza M. Realistic wave conditions and their influence on quantifying the tidal stream energy resource. Appl Energy 2014;136:495–508.
[51] Mason-Jones A, O'doherty DM, Morris CE, O'doherty T. Influence of a velocity profile & support structure on tidal stream turbine performance. Renew Energy 2013;52:23–30.
[52] Georgilakis PS. Technical challenges associated with the integration of wind power into power systems. Renew Sustain Energy Rev 2008;12(3):852–63.
[53] Fairley I, Smith HCM, Robertson B, Abusara M, Masters I. Spatio-temporal variation in wave power and implications for electricity supply. Renew Energy 2017;114:154–65.
[54] Blavette A, O'Sullivan DL, Lewis AW, Egan MG. May. Impact of a wave farm on its local grid: Voltage limits, flicker level and power fluctuations. In: OCEANS, 2012-Yeosu. IEEE; 2012. p. 1–9.
[55] Kovaltchouk T, Armstrong S, Blavette A, Ahmed HB, Multon B. Wave farm flicker severity: Comparative analysis and solutions. Renew Energy 2016;91:32–9.
[56] Potter CW, Negnevitsky M. Very short-term wind forecasting for Tasmanian power generation. IEEE Trans Power Syst 2006;21(2):965–72.
[57] Rahimi E, Rabiee A, Aghaei J, Muttaqi KM, Nezhad AE. On the management of wind power intermittency. Renew Sustain Energy Rev 2013;28:643–53.
[58] Ren G, Liu J, Wan J, Guo Y, Yu D. Overview of wind power intermittency: Impacts, measurements, and mitigation solutions. Appl Energy 2017;204:47–65.
[59] Neill SP, Angeloudis A, Robins PE, Walkington I, Ward SL, Masters I, Lewis MJ, Piano M, Avdis A, Piggott MD, Aggidis G. Tidal range energy resource and optimization–Past perspectives and future challenges. Renew Energy 2018;127:763–78.
[60] Liu Y, Warner T, Liu Y, Vincent C, Wu W, Mahoney B, Swerdlin S, Parks K, Boehnert J. Simultaneous nested modeling from the synoptic scale to the LES scale for wind energy applications. J Wind Eng Ind Aerodyn 2011;99(4):308–19.
[61] Saqib MA, Saleem AZ. Power-quality issues and the need for reactive-power compensation in the grid integration of wind power. Renew Sustain Energy Rev 2015;43:51–64.
[62] Robins PE, Neill SP, Lewis MJ, Ward SL. Characterising the spatial and temporal variability of the tidal-stream energy resource over the northwest European shelf seas. Appl Energy 2015;147:510–22.